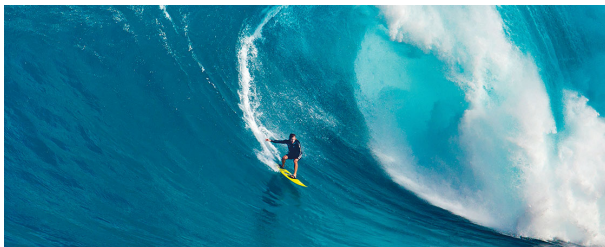


An analytical optimization of plasma density profiles for downramp injection in LWFA

Gaetano Fiore, Università “Federico II”, and INFN, Napoli

7th EAAC, La Biodola Bay, Isola d'Elba, 21-27 Sept 2025



Joint work with: [P. Tomassini](#), ELI-NP, Magurele, Romania

Outline

① Introduction

② Setup & Plane model

Rephrasing plasma kinematics

Plane collisionless multistream plasma model

Special case: the initial density n_{e0} is uniform

Hydrodynamic regime up to wave-breaking

③ Maximizing early WFA of (self-)injected electrons in 4 steps

Motion of a test electron in the plasma wave

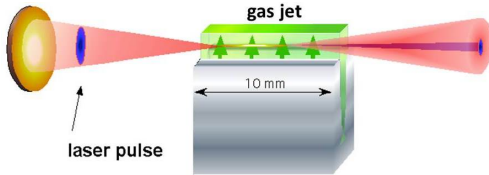
Self-injection and maximal WFA by fixing n_{e0} in 4 steps

3D effects, discussion and conclusions

④ References

Introduction

Laser Wake-Field Acceleration (WFA) [Tajima, Dawson 79] is the first and prototypical mechanism of extreme acceleration of charged particles along short distances: electrons “surf” a plasma wave (PW) driven by a very short laser pulse, e.g. in a supersonic diluted gas jet.



The dynamics is ruled by Maxwell equations coupled to a kinetic theory for plasma electrons, ions. Today these eqs can be solved via more and more powerful, but very costly, PIC simulations: better to run them after a preliminary selection of the input data via simpler models.

Everybody's Dream: solving direct *and* inverse problem

INPUT: Initial ($t \leq 0$)

- **E, B** of free laser pulse;
- Density profile
 $n_{e0} = n_{p0}$
of plasma at rest;



PIC simulations:
extremely accurate
but very expensive

direct

(Semi)analytical
methods in sim-
plified models:
approximate,
cheap

OUTPUT:

- Motion of electrons & ions
(\Rightarrow densities n_e, n_p) for $t \geq 0$
- **E, B** for $t \geq 0$

Everybody's Dream: solving direct **and** inverse problem

OUTPUT: Initial ($t \leq 0$)

- **E, B** of free laser pulse;
- Density profile
 $n_{e0} = n_{p0}$
of plasma at rest;



PIC: no



?

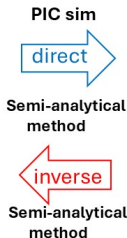
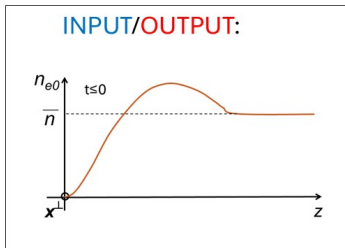
INPUT: for $t \geq 0$

- **Desired Motion of electrons:**
high acceleration, short
bunch, low energy spread,
low emittance, stability...

More modest aim here: solving direct and inverse **plane** problem

INPUT: slowly modulated $\mathbf{E} = \boldsymbol{\varepsilon}^\perp(ct-z)$, $\mathbf{B} = \mathbf{k} \times \mathbf{E}^\perp$ for $t \leq 0$,

e.g. $\boldsymbol{\varepsilon}^\perp(\xi) = a_0 \exp[-\xi^2/2\ell^2] kmc^2/e \times \mathbf{i} \sin k\xi$,



OUTPUT/INPUT: for $t \geq 0$

- Motion (WLs) of electrons
- $\mathbf{A}^\perp(t,z)$, $E^z(t,z)$ \Rightarrow

$$\mathbf{E} = -\partial_0 \mathbf{A}^\perp(t,z) + \mathbf{k} E^z(t,z)$$

$$\mathbf{B} = \nabla \times \mathbf{A}^\perp(t,z)$$

Main goal: maximize early WFA of e^- bunches self-injected in the PW by the 1st WB at the density downramp

Can we learn something useful also for 3D?

Given a very short & intense plane-wave laser pulse $\epsilon^\perp(ct-z)$, here we propose a multi-step preliminary analytical procedure to tailor the initial plasma density $n_{e0}(z)$ to the pulse, so as to control:



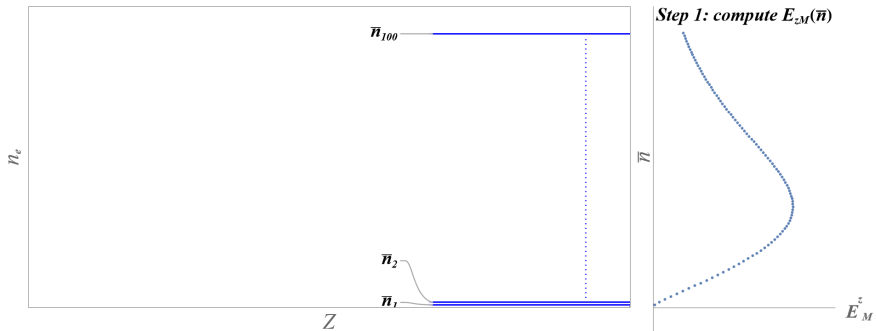
- ① the formation of the plasma wave (PW);
- ② its wave-breaking (WB) at density inhomogeneities; ;
- ③ the self-injection of low-charge bunches of plasma electrons in the PW by the first WB at the density down-ramp;
- ④ to maximize the initial stages of the LWFA of the latter.

We use a **fully relativistic multi-stream, collisionless plane model**, valid as long as no significant change of the ponderomotive force by the pulse.

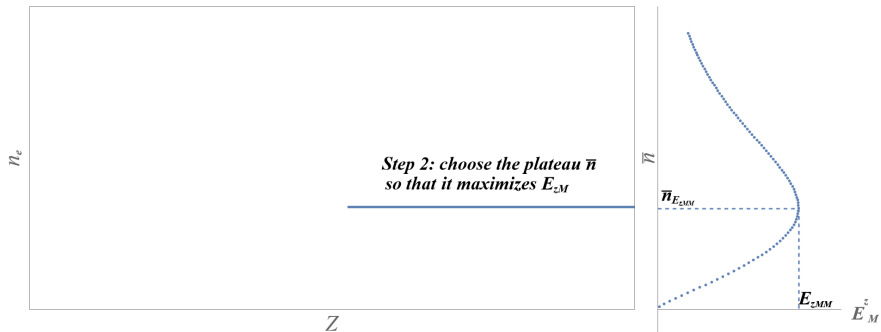
1. Determine n_{e0} by inversion formulae. \mapsto 2. Check its effectiveness.
- \mapsto 3. Improve it by fine-tuning, solving again the direct problem \mapsto ...

Finally, we determine the detailed density and energy distribution of the WFA electrons by FB-PIC simulations.

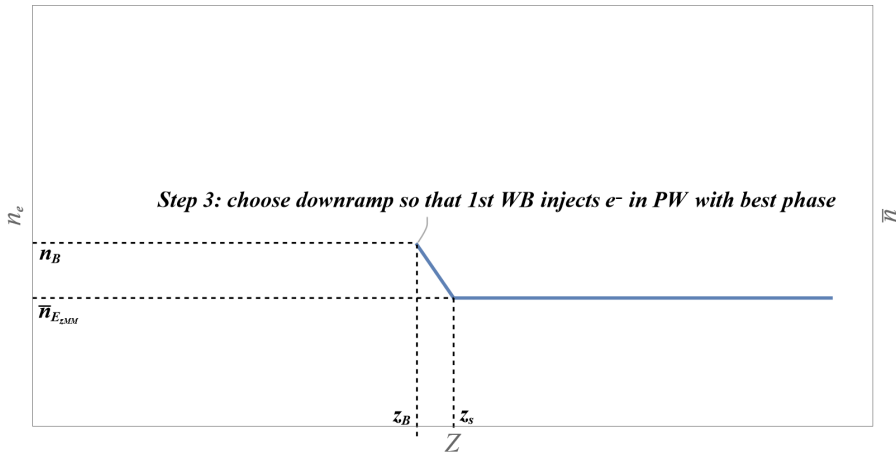
Step 1



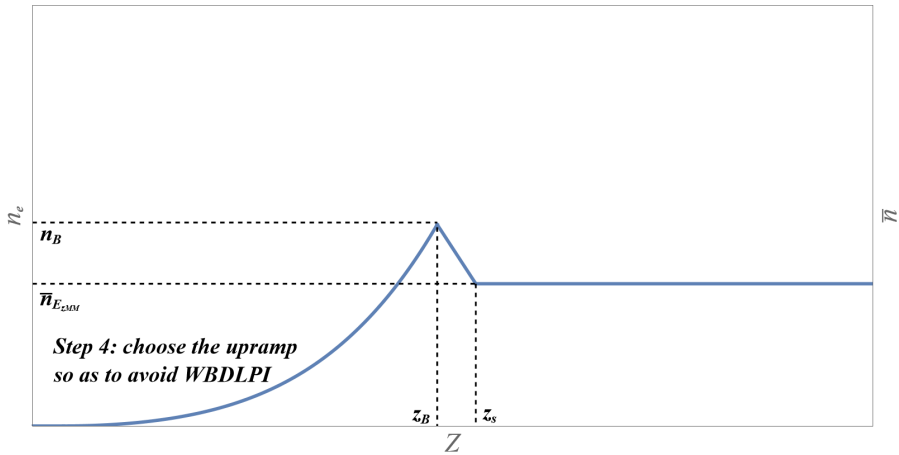
Step 2



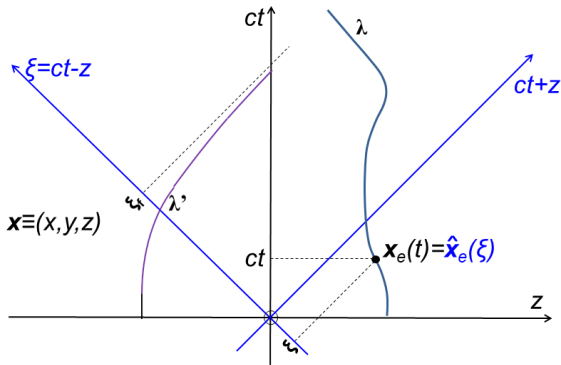
Step 3



Step 4

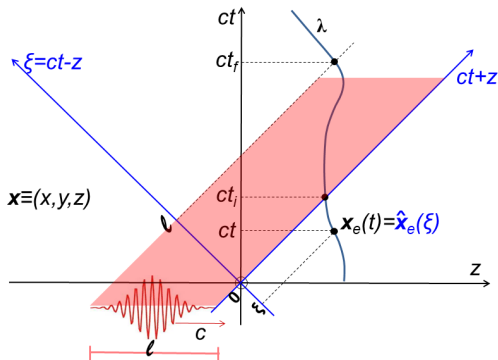


Setup & Plane model



$\xi = ct - z$ can replace t as the independent parameter along the worldline (WL) λ (in Minkowski space) of any massive particle and in its eq. of motion (EoM). Clock=pulse. WL λ' : $v^z \rightarrow c$ as $t \rightarrow \infty \Leftrightarrow \xi \rightarrow \xi_f < \infty$.

We use: CGS units; dimensionless $\beta \equiv \dot{\mathbf{x}}/c$, $\gamma \equiv 1/\sqrt{1-\beta^2}$, 4-velocity $u = (u^0, \mathbf{u}) \equiv (\gamma, \gamma\boldsymbol{\beta}) = \left(\frac{p^0}{mc^2}, \frac{\mathbf{p}}{mc}\right)$, $s \equiv \gamma - u^z > 0$. $s \rightarrow 0$ implies $u^z \rightarrow \infty$.



How to simplify the Lorentz EOM

$$\dot{\mathbf{p}}(t) = q \epsilon^\perp[ct - z(t)] + \mathbf{k} q E^z(t, z) + (q/c) \mathbf{v}(t) \times \{ \mathbf{k} \times \epsilon^\perp[ct - z(t)] \} \quad ? \quad (1)$$

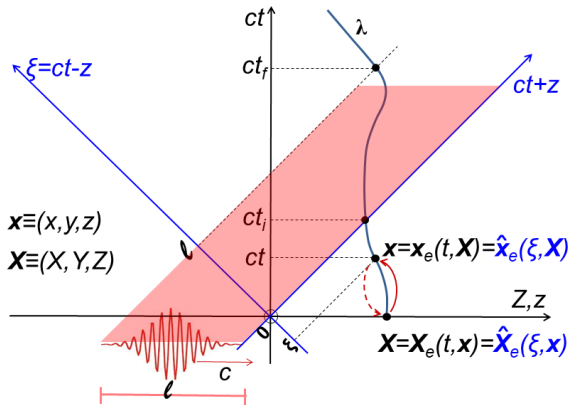
Changing variables $t \mapsto \xi$, $p^z \mapsto p^- \equiv p^0/c - p^z = mc s$ transforms (1) into

$$\hat{\mathbf{p}}^{\perp'}(\xi) = q \epsilon^\perp(\xi)/c, \quad \hat{s}'(\xi) = \frac{-q}{mc^2} \check{E}^z(\xi, \hat{z}) \quad (2)$$

($\epsilon^\perp \not\propto$ unknown $z(t)$). If $E^z = 0$ and $\mathbf{p}(0) = 0$ these are immediately solved by $s = 1$, $\hat{\mathbf{p}}^\perp(\xi) = (q/c) \int_{-\infty}^{\xi} d\zeta \epsilon^\perp(\zeta) =: (-q/c) \alpha^\perp(\xi)$, $\Rightarrow p^z = \mathbf{p}^{\perp 2}/2mc$.

Rephrasing plasma kinematics

We regard ions as immobile. No collisions \Rightarrow : all e^- having the same position \mathbf{X} and velocity \mathbf{V} at $t = 0$ will have the same position $\mathbf{x}_e(t, \mathbf{X}, \mathbf{V})$ and velocity $\dot{\mathbf{x}}_e(t, \mathbf{X}, \mathbf{V})$ at $t > 0$. Since here $\mathbf{V} = \mathbf{0}$ for all e^- , then $\mathbf{x}_e = \mathbf{x}_e(t, \mathbf{X})$. The *hydrodynamic regime* (HR) lasts as long as $\mathbf{X} \mapsto \mathbf{x}$ are 1-to-1, i.e. WLs do not intersect. Afterwards: *multistream* or *post-hydrodynamic regime* (PHR).



HR: Eulerian observable $f(t, \mathbf{x}) = \check{f}(\xi, \mathbf{x}) = \tilde{f}(t, \mathbf{X}) = \hat{f}(\xi, \mathbf{X})$ Lagrangian obs. ↻ 🔍

Plane collisionless multistream plasma model

Transverse plane symmetry implies:

Eulerian fields can depend only on t, z ;

their Lagrangian counterparts and the displacements

$\Delta_e \equiv \mathbf{x}_e(t, \mathbf{X}) - \mathbf{X}$ can depend only on t, Z ;

their “hatted” Eulerian/Lagrangian counterparts can depend only on ξ, z , resp. ξ, Z .

The rigid motion of each electrons' **transverse sheet** (=very thin layer) is codified by $z_e(t, Z)$ [or $\hat{z}_e(\xi, Z)$].

Different sheets may cross each other [Dawson62]; the HR lasts as long as this does not occur.

Maxwell eqs

$$\nabla \cdot \mathbf{E} = 4\pi j^0, \quad \frac{1}{c} \partial_t E^Z + 4\pi j^Z = (\nabla \wedge \mathbf{B})^Z = 0 \quad (3)$$

with the above initial conditions are solved by [GF,PT25]

$$E^Z(t, z) = 4\pi e [\tilde{N}(z) - N_e(t, z)], \quad (4)$$

$$\tilde{N}(z) \equiv \int_0^z d\zeta n_{e0}(\zeta), \quad N_e(t, z) \equiv \int_0^\infty dZ \tilde{n}_0(Z) \theta[z - z_e(t, Z)]; \quad (5)$$



$j^0(t, z) = e[n_{e0}(z) - n_e(t, z)]$, $\mathbf{j} = -en_e \mathbf{v}_e$ are the el. charge density and current density; $\tilde{N}(z)$, $N_e(t, z)$ are the # (protons), # (electrons) per unit transv. surface with $z' \leq z$ at time t . j^μ diverge at WB, N_e does not: (4) ‘regularizes’ (3).

Simplest gauge choice: also $A = (A^0, \mathbf{A})$ depends only on t, z , and

$$\mathbf{A}^\perp(t, z) \equiv -c \int_{-\infty}^t dt' \mathbf{E}^\perp(t', z) \quad (\text{physical observable}); \quad (6)$$

Since $\mathbf{u}_e^\perp(0, \mathbf{x}) = \mathbf{0}$, Lorentz eq. implies $\mathbf{u}_e^\perp = e\mathbf{A}^\perp/mc^2$.

$$\text{For } t \leq 0 \quad \mathbf{A}^\perp(t, z) = \alpha^\perp(ct - z), \quad \alpha^\perp(\xi) \equiv - \int_{-\infty}^{\xi} d\zeta \epsilon^\perp(\zeta). \quad (7)$$

We can reformulate Maxwell eq. $\square \mathbf{A}^\perp = 4\pi \mathbf{j}^\perp$ as the integral eq.

$$\mathbf{A}^\perp(t, z) - \alpha^\perp(ct - z) = -\frac{K}{2} \int d\eta d\zeta \theta(\eta) \theta(ct - \eta - |z - \zeta|) \left(\frac{n_e \mathbf{A}^\perp}{\gamma_e} \right)(\eta, \zeta), \quad (8)$$

$K \equiv \frac{4\pi e^2}{mc^2}$. Neglecting pulse evolution, $\mathbf{A}^\perp(t, z) = \alpha^\perp(ct - z)$. The remaining eqs to solve is the family (parametrized by Z) of ordinary Cauchy problems

$$\hat{z}'_e(\xi, Z) = \frac{1 + v(\xi)}{2\hat{s}^2(\xi, Z)} - \frac{1}{2}, \quad (9)$$

$$\hat{s}'(\xi, Z) = \frac{e\check{E}^z}{mc^2} = K \left\{ \tilde{N}[\hat{z}_e(\xi, Z)] - \int_0^\infty d\zeta n_{e0}(\zeta) \theta[\hat{z}_e(\xi, Z) - \hat{z}_e(\xi, \zeta)] \right\}, \quad (10)$$

$$\hat{z}_e(0, Z) = Z, \quad \hat{s}(0, Z) = 1, \quad (11)$$

in the unknowns $\hat{s}(\xi, Z)$, $\hat{z}_e(\xi, Z)$. Here $v(\xi) \equiv (e\alpha^\perp(\xi)/mc^2)^2$.

HR: dynamics reduced to decoupled Hamilton eqs for 1df

As long as the HR holds, eqs (9-11) for different Z 's *decouple* and become eqs

$$\hat{\Delta}' = \frac{1+\nu}{2\hat{s}^2} - \frac{1}{2}, \quad \hat{s}' = \kappa \left\{ \tilde{N}[Z+\hat{\Delta}] - \tilde{N}(Z) \right\}, \quad (12)$$

$$\hat{\Delta}(0, Z) = 0, \quad \hat{s}(0, Z) = 1 \quad (13)$$

[GF18] in the unknowns $\hat{\Delta}(\xi, Z) \equiv \hat{z}_e(\xi, Z) - Z$, $\hat{s}(\xi, Z)$, $\hat{s}(\xi, Z)$. For each $Z \geq 0$ (12) are **Hamilton equations** $q' = \partial \hat{H} / \partial p$, $p' = -\partial \hat{H} / \partial q$ of a **1-dim system**: $\xi, \hat{\Delta}, -\hat{s}$ play the role of t, q, p , and the Hamiltonian up to mc^2 reads

$$\begin{aligned} \hat{H}(\hat{\Delta}, \hat{s}, \xi; Z) &:= \frac{\hat{s}^2 + 1 + \nu(\xi)}{2\hat{s}} + \mathcal{U}(\hat{\Delta}; Z), \\ \mathcal{U}(\Delta; Z) &:= \kappa \int_0^\Delta d\zeta (\Delta - \zeta) n_{e0}(Z + \zeta). \end{aligned} \quad (14)$$

For $\xi > l$ $\nu = \text{const}$, $\hat{H} = h(Z) = \text{const}$, (12) are autonomous and **can be solved by quadrature**; if $Z > 0$ the solutions are periodic in ξ ; $\xi_H(Z) \equiv \text{period}$.

All other unknowns can be expressed via $(\hat{\Delta}, \hat{s})$:

$$\hat{\mathbf{u}}^\perp = \frac{e \alpha^\perp(\xi)}{mc^2}, \quad \hat{u}^z = \frac{1 + \hat{\mathbf{u}}^{\perp 2} - \hat{s}^2}{2\hat{s}}, \quad \hat{\gamma} = \frac{1 + \hat{\mathbf{u}}^{\perp 2} + \hat{s}^2}{2\hat{s}}, \quad (15)$$

$$\hat{\mathbf{x}}_e^\perp(\xi, \mathbf{X}) - \mathbf{X}^\perp = \int_0^\xi d\eta \frac{\hat{\mathbf{u}}^\perp(\eta)}{\hat{s}(\eta, Z)}, \quad \hat{z}_e(\xi, \mathbf{X}) - Z = \hat{\Delta}(\xi, Z). \quad (16)$$

Special case: $n_{e0}(Z) \equiv \bar{n} = \text{const}$

If $n_{e0}(Z) \equiv \bar{n} = \text{const}$, then (12) and its solution are in fact **Z-independent**:

$$\Delta' = \frac{1+\nu}{2s^2} - \frac{1}{2}, \quad s' = M\Delta, \quad \Delta(0)=0, \quad s(0)=1, \quad (17)$$

$M \equiv K\bar{n} = \frac{\omega_p^2}{c^2}$, $\mathcal{U}(\Delta, Z) = \frac{M}{2}\Delta^2$: relativistic harmonic oscillator. $h(Z; n_{e0}) = \bar{h}(\bar{n})$.

a) Linearly polarized gaussian pulse with peak amplitude $a_0 \equiv \lambda e E_M^\perp / 2\pi m c^2 = 2$, $l_{fwhm} = 10\lambda$. We consider $l = 40\lambda$ and cut tails outside $|\xi - l/2| < l/2$.

b) Corresponding solution of (17) if $n_{e0}(z) = \bar{n}^j \equiv n_{cr}/268$ ($n_{cr} = \pi m c^2 / e^2 \lambda^2$ is the critical density); as a result, $E/mc^2 \equiv h = 1.28$.

\hat{s} is insensitive to fast oscillations of ϵ^\perp !

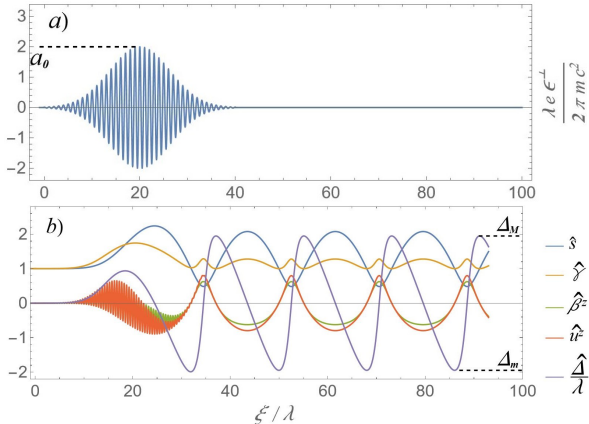


Figure 1

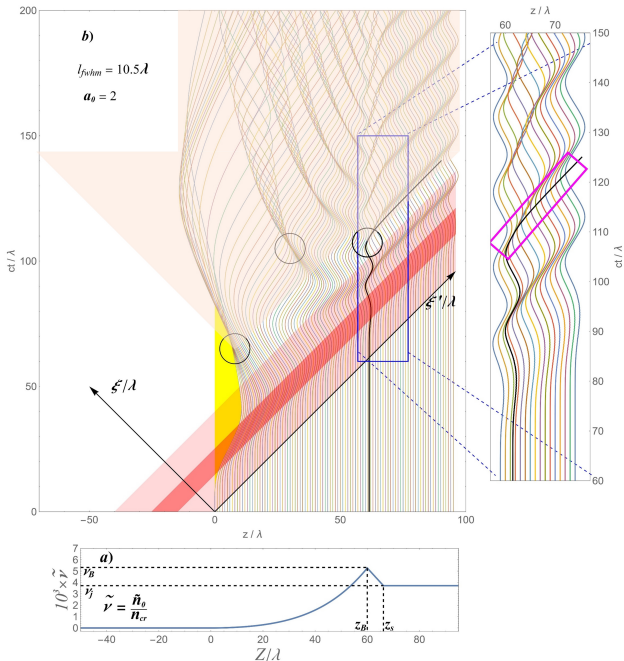
a) An “optimal” $n_{e0}(z)$ for the above pulse: $\bar{n} = \bar{n}^j = n_{cr}/268$, $n_b = 1.32 \times \bar{n}^j$, $n_B = 1.42 \times \bar{n}^j$, $z_B = 60\lambda$, $z_s - z_B = 6.2\lambda$.

b) WLs of e^- with $Z = 0, \lambda, \dots, 95\lambda$ are as plot until they first intersect (circles) \Rightarrow WBs.

Black WL: e^- self-injected by the 1st WB; is Ok for all t .

Nearly maximal $F = 0.286$. If $\lambda = 0.8\mu\text{m}$, this leads to a remarkable energy gain of 0.182MeV per μm .

c) Zoom of blue box.



Hydrodynamic regime up to wave-breaking

The HR holds as long as $\hat{J} \equiv \left| \frac{\partial \hat{x}_e}{\partial \mathbf{x}} \right| = \frac{\partial \hat{z}_e}{\partial Z} > 0$. For $\xi > l$ [GF et al 23]

$$\hat{J}(\xi + k\xi_H, Z) = \hat{J}(\xi, Z) - k \frac{\partial \xi_H}{\partial Z} \Delta'(\xi, Z), \quad \forall k \in \mathbb{N}, Z \geq 0, \quad (18)$$

$$\Leftrightarrow \hat{J}(\xi, Z) = a(\xi, Z) + \xi b(\xi, Z), \quad (19)$$

where $b \equiv -\frac{\partial \log \xi_H}{\partial Z} \hat{\Delta}'$, $a \equiv \hat{J} - \xi b$ are ξ_H -periodic in ξ , and b has zero mean over a period (apply ∂_Z to $\Delta[\xi + n\xi_H(Z), Z] = \Delta(\xi, Z)$, use ξ_H -periodicity of Δ').

By (18) we can extend our knowledge of \hat{J} from $[l, l + \xi_H[$ to all $\xi \geq l$.

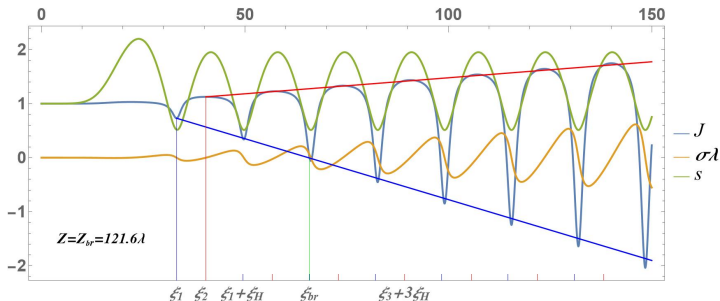


Figure 3: $\hat{J}, \hat{\sigma}$ vs. ξ for $Z = Z_b \simeq 121.6\lambda$ and input data as in Fig. 2.

Maximizing the WFA of (self-)injected e^-

Motion of test electrons in the plasma wave

The eqs for a *test* e^- sheet injected in the PW behind the pulse reduce to

$$\hat{z}'_i(\xi) = \frac{1}{2\hat{s}_i^2(\xi)} - \frac{1}{2}, \quad \hat{s}'_i(\xi) = M\Delta(\xi) \quad (21)$$

along the density plateau, and $\hat{s}_i(\xi) - s(\xi) = \delta s \equiv s_{i0} - s(\xi_0) = \text{const}$, cf (17b).
If $\delta s < -s_m$ (**trapping condition**), then $\exists \xi_f > \xi_0$ s.t. $\hat{s}_i(\xi_f) = 0$, e^- is **trapped & accelerated in a trough of the PW**. As $t \rightarrow \infty$

$$z_i \sim ct, \quad \gamma_i \simeq F z_i / \lambda \xrightarrow{z_i \rightarrow \infty} \infty, \quad (22)$$

$F \equiv K \bar{n} \lambda |\Delta(\xi_f)|$; reliable as long as pulse depletion is negligible: $z_i \leq z_{pd}$.

Fixed \bar{n} , if $\delta s = -1$, then $|\Delta(\xi_f)| = |\Delta_m| = \Delta_M$, and F is maximal:

$$\gamma_i(z_i; \bar{n}) \simeq \sqrt{j(\bar{n})} z_i / \lambda, \quad (23)$$

$$j(\bar{n}) \equiv \bar{n} [\bar{h}(\bar{n}) - 1] 8\pi^2 / n_{cr}, \quad (24)$$

where $\bar{h}(\bar{n}) =$ final energy transferred by the pulse to the plateau plasma e^- .

Physically, $|\Delta(\xi_f)| = \Delta_M$ means that the test sheet tends to the transverse plane of the travelling bucket where $-E^z$ is maximal. Below $\nu \equiv n_0 / n_{cr}$.

Self-injection & maximal WFA by fixing n_{e0} in 4 steps

Step 1: Computing $\bar{h}(\nu), j(\nu)$.

(We interpolate 200 points; few seconds via *Mathematica*).

Step 2: Optimal plateau density \bar{n} .

If the depth available for WFA is $z_i \leq z_{pd}(\nu_j)$, set $\bar{n}/n_{cr} = \nu_j \equiv \max\{j(\nu)\}$:

$$\gamma_i^M(z_i) \simeq \sqrt{j(\nu_j)} z_i / \lambda. \quad (25)$$

Step 3: n_{e0} with optimal down-ramp for self-injection, LWFA.

$$n_{e0}(Z) = \bar{n} + \Upsilon(Z - z_s), \quad z_B \leq Z \leq z_s,$$

$\Upsilon = \frac{\bar{n} - n_B}{z_s - z_B}$. Let (ξ_b, Z_b) be the pair (ξ, Z) with smallest ξ s.t. $\hat{J}(\xi, Z) = 0$. The Z_b e^- are the fastest injected & trapped in a PW trough by the 1st WB. We fix Υ, z_B requiring: $\delta s = -1$, so that (23) applies; no WBDLPI.

Step 4: Choosing an up-ramp of n_{e0}

out of the ∞ -ly many ones growing from 0 to n_B and preventing WB for $\xi < \xi_b$; $n_{e0}(z) \simeq O(z^2)$ [GF et al

2022-23].

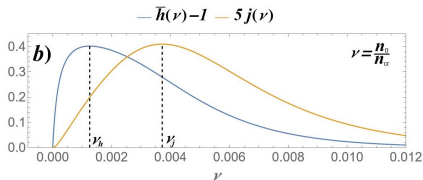


Figure 4: $\bar{h}-1$ (energygain per plasma e^-) and j by the pulse of fig. 1a, vs. ν

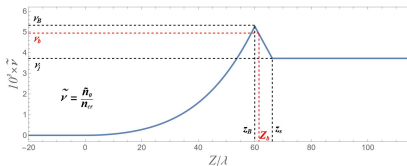


Figure 5: Optimal density associated to the pulse of fig. 1a, used in fig. 2.

3D effects, discussion and conclusions

Summarizing, the steps of our preliminary optimization process are:

- ① finding the final energy \bar{h} transferred by the pulse to the plateau plasma electrons and $j = 8\pi^2 [\bar{h} - 1] \bar{n} / n_{cr}$ as functions of the density \bar{n} ;
- ② finding the 'optimal' value \bar{n}^j of \bar{n} maximizing $j(\bar{n})$, i.e. $E_M^z(\bar{n})$;
- ③ finding the 'optimal' length $z_B - z_s$ and slope Υ of the density down-ramp;
- ④ adjusting the up-ramp ($z < z_B$) of $n_{e0}(z)$ to avoid WB for $\xi < \xi_b$.

Range of applicability of the model?

Depletion and change of ponderomotive force by the pulse are negligible for

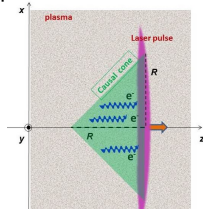
$$\frac{z}{l'} \frac{4}{a_0^2} \frac{\bar{n}}{n_{cr}} [\bar{h}(\bar{n}) - 1] \ll 1 \quad (26)$$

Pulse cylindrically symmetric around \vec{z} with waist R : by causality our results hold strictly in the green causal cone trailing the pulse, approximately nearby.

In particular, if the pulse has maximum at $\xi = \frac{l}{2}$, and

$$R > \xi_b - \frac{l}{2}, \quad R \gg \frac{a_0 \lambda}{2\pi} [\bar{h} + \sqrt{\bar{h}^2 - 1}] \quad (27)$$

then the $\mathbf{X} \simeq (0, 0, Z_b) e^-$ keep in that cone and move as above: same maximal WFA, as far as pulse not depleted. ▶



Apply our optimization procedure to the pulse of Fig. 1a ($a_0=2$, $I_{fwhm}=10\lambda$): we find the initial density $n_{e0}(z)$ and the WLs of Fig. 2a; $F=0.28$.
 Ti-Sa laser: $\lambda \simeq 0.8\mu\text{m}$; peak intensity $\mathcal{I}=1.7\times 10^{19}\text{W}/\text{cm}^2$, $\bar{n}^j=6.5\times 10^{18}\text{cm}^{-3}$ yields the **remarkable energy gain of 0.182MeV per μm** of the Z_b electrons (black WL). Very good agreement with FB-PIC simulations (by P. Tomassini):

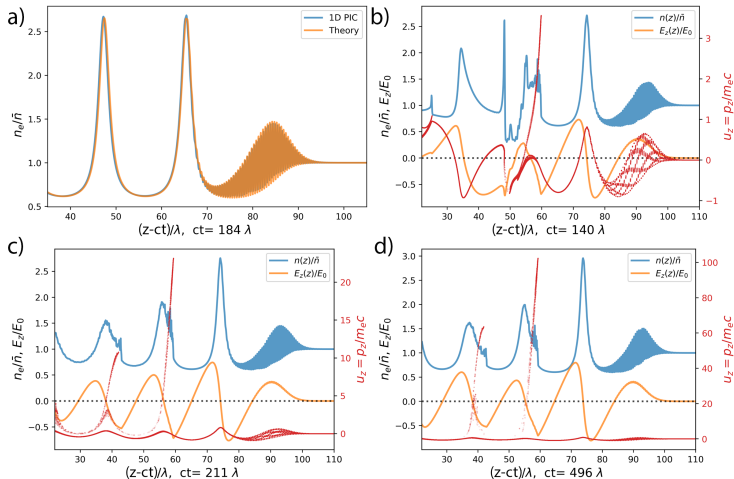


Figure 6: FB-PIC (1D equivalent) simulations run with input data of fig. 2a.

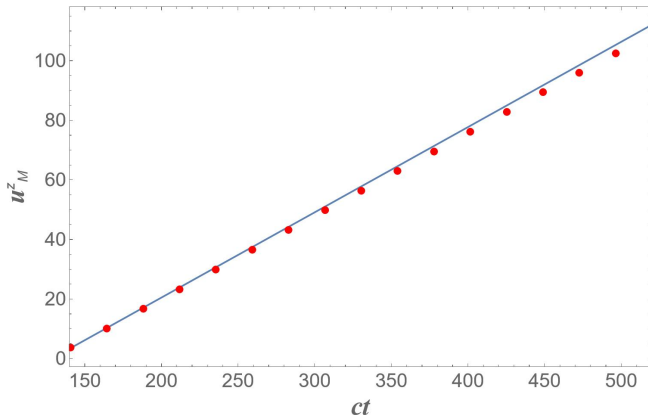












Figure 7: Comparison between semi-analytical model and FB-PIC (1D equivalent) simulations run with the same input: Maximum longitudinal momentum obtained by the PIC simulation (red circles) and prediction from the theory (blue line).

References

-  G. Fiore, P. Tomassini, *Analytical optimization of plasma density profiles for downramp injection in laser wake-field acceleration*, arXiv:2506.06814.
-  G. Fiore, *A preliminary analysis for efficient laser wakefield acceleration*. IEEE 20th Advanced Accelerator Concepts workshop (AAC22), Naperville, Nov. 6-11, 2022. <https://doi.org/10.1109/AAC55212.2022.10822960>
-  G. Fiore, T. Akhter, S. De Nicola, R. Fedele, D. Jovanović, Phys. D: Nonlinear Phenom., **454** (2023), 133878.
-  G. Fiore, M. De Angelis, R. Fedele, G. Guerriero, D. Jovanović, Mathematics **10** (2022), 2622; Ricerche Mat. (2023).
-  G. Fiore, P. Catelan, Nucl. Instr. Meth. Phys. Res. **A909** (2018), 41-45.
-  G. Fiore, J. Phys. A: Math. Theor. **51** (2018), 085203.
-  G. Fiore, J. Phys. A: Math. Theor. **47** (2014), 225501.
-  G. Fiore, R. Fedele, U. de Angelis, Phys. Plasmas **21** (2014), 113105.
-  G. Fiore, S. De Nicola, Phys. Rev. Acc. Beams **19** (2016), 071302 (15pp).
-  G. Fiore, Ricerche Mat. **65** (2016), 491-503.